Eleventh U.S. National Conference on Earthquake Engineering
Integrating Science, Engineering & Policy
June 25-29, 2018
Los Angeles, California

EXPERIMENTAL AND NUMERICAL INVESTIGATIONS ON SEISMIC APPLICATIONS OF HIGH DAMPING SMAS

F. Shi[1], G. P. Toker[2], F. S. Dizaji[3], O. E. Ozbulut[4] and H. E. Karaca[5]

ABSTRACT

There are several different mechanisms for creating a restoring force to return a building structure to plumb after an earthquake. One approach is to allow structure to undergo controlled rocking at discrete locations such as column-base joint or beam-column joints. Another approach is to employ braces or seismic control devices with self-centering capabilities. Due to its inherent nonlinear elastic behavior, shape memory alloys (SMAs) have been considered to develop self-centering braces or devices. Recently, NiTiHfPd alloys that have very high strength (up to 2000 MPa), high dissipation/damping capacity, good cyclic stability and large operating temperature have been developed. This study explores the superelastic response of NiTiHfPd SMAs under various conditions and illustrates their application into seismic applications. In order to collect experimental data, uniaxial tests are conducted on superelastic NiTiHfPd SMAs in the temperature range of -35 ºC to 25 ºC, and at the loading frequencies of 0.05 Hz to 1 Hz with four different strain amplitudes. The effects of loading rate and temperature on superelastic characteristics of NiTiHfPd SMAs are examined. A numerical model that reliably simulates the response of NiTiHfPd SMAs is developed. Then, a four-story moment resisting frame with and without supplementary SMA damping elements is designed and modeled. Nonlinear response history analyses are conducted to assess the performance of NiTiHfPd SMAs in mitigating seismic response and limiting residual drifts of steel frames subjected to strong ground motions.

[1] Graduate Student Researcher, Dept. of Civil Eng., Guangzhou University, Guangzhou, 510006, China
[2] Graduate Student Researcher, Dept. of Mechanical Engineering, University of Kentucky, Lexington, KY, 40502
[3] Graduate Student Researcher, Dept. of Civil Engineering, University of Virginia, Charlottesville, VA 22901
[4] Assistant Professor, Dept. of Civil and Environmental Engineering, University of Virginia, Charlottesville, VA 22901 (email: ozbulut@virginia.edu)
[5] Associate Professor, Dept. of Mechanical Engineering, University of Kentucky, Lexington, KY, 40502

Shi F, Toker GP, Dizaji FS, Ozbulut OE, Karaca, HE. Experimental and Numerical Investigations on Seismic Applications of High Damping SMAs. *Proceedings of the 11th National Conference in Earthquake Engineering*, Earthquake Engineering Research Institute, Los Angeles, CA. 2018.

Eleventh U.S. National Conference on Earthquake Engineering
Integrating Science, Engineering & Policy
June 25-29, 2018
Los Angeles, California

Experimental and Numerical Investigations on Seismic Applications of High Damping SMAs

F. Shi[1], G. P. Toker[2], F. S. Dizaji[3], O. E. Ozbulut[4] and H. E. Karaca[5]

ABSTRACT

There are several different mechanisms for creating a restoring force to return a building structure to plumb after an earthquake. One approach is to allow structure to undergo controlled rocking at discrete locations such as column-base joint or beam-column joints. Another approach is to employ braces or seismic control devices with self-centering capabilities. Due to its inherent nonlinear elastic behavior, shape memory alloys (SMAs) have been considered to develop self-centering braces or devices. Recently, NiTiHfPd alloys that have very high strength (up to 2000 MPa), high dissipation/damping capacity, good cyclic stability and large operating temperature have been developed. This study explores the superelastic response of NiTiHfPd SMAs under various conditions and illustrates their application into seismic applications. In order to collect experimental data, uniaxial tests are conducted on superelastic NiTiHfPd SMAs in the temperature range of -35 ºC to 25 ºC, and at the loading frequencies of 0.05 Hz to 1 Hz with four different strain amplitudes. The effects of loading rate and temperature on superelastic characteristics of NiTiHfPd SMAs are examined. A numerical model that reliably simulates the response of NiTiHfPd SMAs is developed. Then, a four-story moment resisting frame with and without supplementary SMA damping elements is designed and modeled. Nonlinear response history analyses are conducted to assess the performance of NiTiHfPd SMAs in mitigating seismic response and limiting residual drifts of steel frames subjected to strong ground motions.

Introduction

In addition to the immediate structural response to a dynamic event, the amount of residual deformation—once motion has stopped—is an important metric to evaluate building post-event performance. Due to its inherent re-centering ability, shape memory alloys (SMAs) have been extensively studied over the past decade to develop self-centering structural systems [1-5].

[1] Graduate Student Researcher, Dept. of Civil Eng., Guangzhou University, Guangzhou, 510006, China and Dept. of Civil and Environmental Eng., University of Virginia, Charlottesville, VA, 22901
[2] Graduate Student Researcher, Dept. of Mechanical Engineering, University of Kentucky, Lexington, KY, 40502
[3] Graduate Student Researcher, Dept. of Civil Engineering, University of Virginia, Charlottesville, VA 22901
[4] Assistant Professor, Dept. of Civil and Environmental Engineering, University of Virginia, Charlottesville, VA 22901 (email: ozbulut@virginia.edu)
[5] Associate Professor, Dept. of Mechanical Engineering, University of Kentucky, Lexington, KY, 40502

Shi F, Toker GP, Dizaji FS, Ozbulut OE, Karaca, HE. Experimental and Numerical Investigations on Seismic Applications of High Damping SMAs. *Proceedings of the 11th National Conference in Earthquake Engineering*, Earthquake Engineering Research Institute, Los Angeles, CA. 2018.

Although the shape memory phenomenon has been observed in a variety of alloys, due its excellent ductility and shape memory properties near equatomic NiTi (49-51 at% Ni) is known as the workhorse of research and applications in SMA related studies. However, NiTi has some limitations such as limited material strength and damping capacity and unsatisfactory shape memory properties (e.g. low recoverable strain) at high stress levels and elevated temperatures [6-7].

Recently, NiTiHfPd SMAs that possess ultra-high strength and superior superelasticity have been developed [8-9]. The use of NiTiHfPd SMAs in a seismic response control device can avoid employing additional energy dissipation unit and/or requiring large quantities of material due to high energy dissipation capabilities and strength of NiTiHfPd. This study first summarizes the experimental testing results on NiTiHfPd SMAs and then explores the seismic performance of steel frame buildings designed with a NiTiHfPd SMA-based bracing system. In particular, the response of SMA-braced frame at different seismic intensity levels are evaluated and compared with a traditionally designed steel moment resisting frame (SMRF). The effect of temperature on the seismic performance of the SMA-braced frame is also analyzed.

Experimental Testing of NiTiHfPd SMAs

For experimental characterization, induction melted $Ni_{45.3}Ti_{29.7}Hf_{20}Pd_5$ (at %) alloys are used. The sample dimensions are 4x4x8mm^3. The sample is heat treated at 400 ^{o}C for 3 hours and then water quenched before testing. Mechanical tests are performed using a 100 kN MTS Landmark servo-hydraulic test frame. Loading and unloading are conducted at the selected frequencies of 0.05, 0.5 and 1Hz and temperatures of -35 ^{o}C, 5 ^{o}C and 25 ^{o}C. The strain is measured by an MTS high-temperature extensometer with a gauge length of 12 mm and K-type thermocouples are used to monitor the temperature during the test.

Experimental Results

Fig. 1(a) to (c) show strain-stress curves of NiTiHfPd SMAs at -35 °C, 5 °C and 25 °C, respectively. The curves at each temperature are plotted for the tests conducted at different strain amplitudes and different loading frequencies. It can be seen that the hystersis loops of NiTiHfPd SMAs move upward with increasing tempreture. In addition, when tempreture decreases from 25 °C to -35 °C, the hystersis loops tend to have a wider area. This indicates that energy dissipation of the SMA increases with a decrease in temperature. Increasing loading frequency also shifts hysteresis loops upward, yet, it does not change the area of hysteresis loops considerably.

In order to enable the assessment of the test results in a more quantative way, some important mechanical proporties, including the equivalent (secant) stiffness, K_e, the energy dissipation per cycle, E_D, and the equivalent viscous damping ratio, ξ_{eqv} are calculated. The equivalent viscous damping ratio and the equivalent (secant) stiffness are defined as:

$$\xi_{eqv} = \frac{E_D}{4\pi E_S} \tag{1}$$

$$K_e = \frac{F_{max} - F_{min}}{D_{max} - D_{min}} \tag{2}$$

where E_S is the maximum elastic strain energy for the same cycle; and F_{max} and F_{min} are the

maximum and minimum forces obtained for the maximum and minimum cyclic deformation D_{max} and D_{min}.

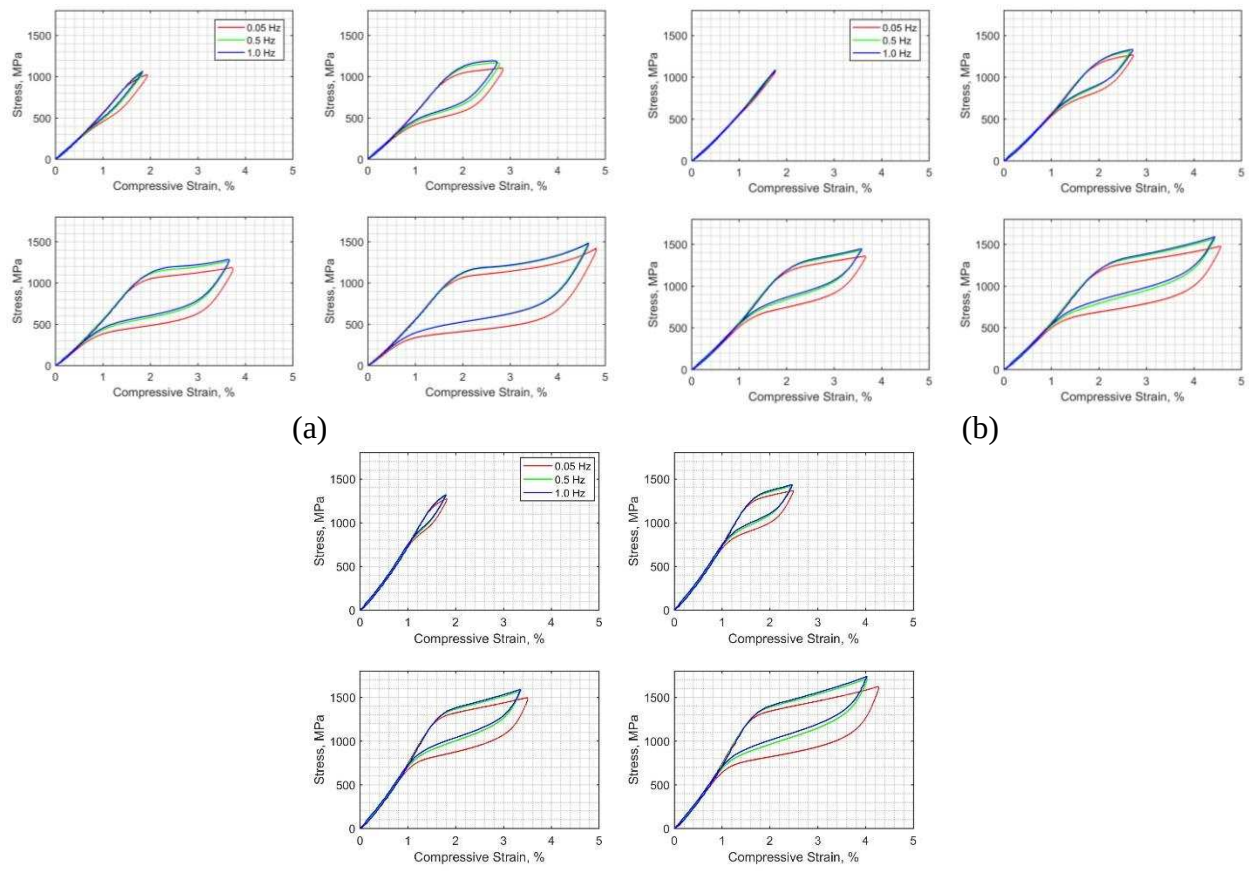


Figure 1. Stress-strain curves of SMAs at different tempretures; (a) -35 °C, (b) 5 °C, and (c) 25 °C with various strain and loading frequency levels

Fig. 2 shows the variation of energy dissipation per cycle, equivalent viscous damping, and equivalent stiffness with tempreture for the tests conducted at different loading frequences. It can be seen that the energy dissipation generally decreases with increasing tempreture. In particular, there is a 32%, 42%, and 50% decrease in the dissipated energy at the loading frequencies of 0.05, 0.5 and 1.0 Hz, respectively when the temperature changes from -35 °C to 25 °C. A similar decrease is also observed in the equivalent viscous damping ratio for increasing tempreture. The equivalent viscous damping ratio decreases from 4.96% at -35 °C to 3.34% at 25 °C at loading frequency of 0.05 Hz; from 4.04% at -35 °C to 2.29% at 25 °C at loading frequency of 0.5 Hz; and from 4.07% at -35 °C to 1.98% at 25 °C at loading frequency of 1 Hz. Despite the significant changes in damping properties observed for a temperature change from -35 °C to 25 °C, the change in both dissipated energy and equivalent viscous damping ratio remain within 10% when the tempreture changes from 5 °C to 25 °C. On the other hand, equivalent stiffness obtains higher values at higher tempretures for various loading frequinces. When tempreture increases from -35 °C to 25 °C, the equivalent stiffness increases by 29%, 34%, and 35% at loading frequencies of 0.05, 0.5, 1 Hz, respectively. This increase in the equivalent stiffness can be attributed to the fact that during loading the material reaches at higher

stress levels for the same strain amplitude at higher temperatures.

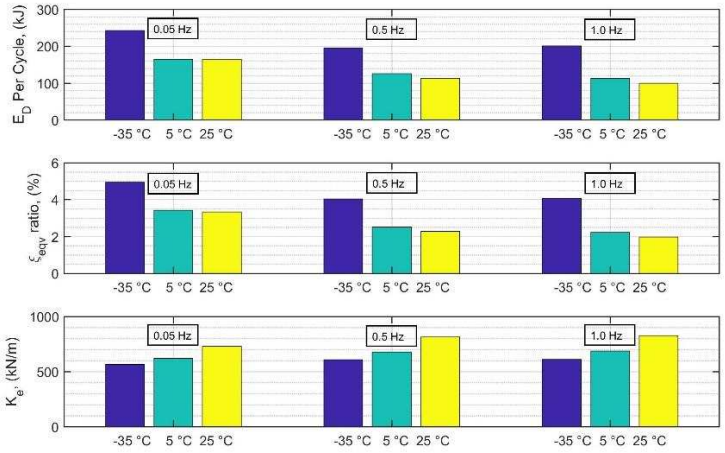


Figure 2. Variation of energy dissipation per cycle, equivalent viscous damping, and equivalent stiffness with tempreture

Fig. 3 shows the variation of energy dissipation per cycle, equivalent viscous damping, and equivalent stiffness with loading frequencies at different tempretures. It can be seen that the reduction in energy dissipation, for various tempretures, ranges from 20% to 31% when the loading frequency increase from 0.05 Hz to 0.5 Hz. Nonetheless, the energy dissipation alters only -10% when loading frequences changes from 0.5 Hz to 1.0 Hz. Similarly, it can be seen that the equivalent viscous damping ratio decreases by increasing loading frequency. In particular, there is a 26% and 11% reduction in the equivalent viscous damping ratio when the loading frequency changes from 0.05 Hz to 0.5 Hz and when the loading frequency alters from 0.5 Hz to 1.0 Hz, respectively. On the other hand, due to an increase observed in the slope of forward phase transformation plateu with an increase in the loading frequency, the equivalent stiffness attains slightly higher values at larger loading frequencies. When the loading frequency increases from 0.05 Hz to 1.0 Hz, the equivalent stiffness increases 8%, 10%, and 13% at test tempretures of 35 °C, 5 °C to 25 °C, respectively.

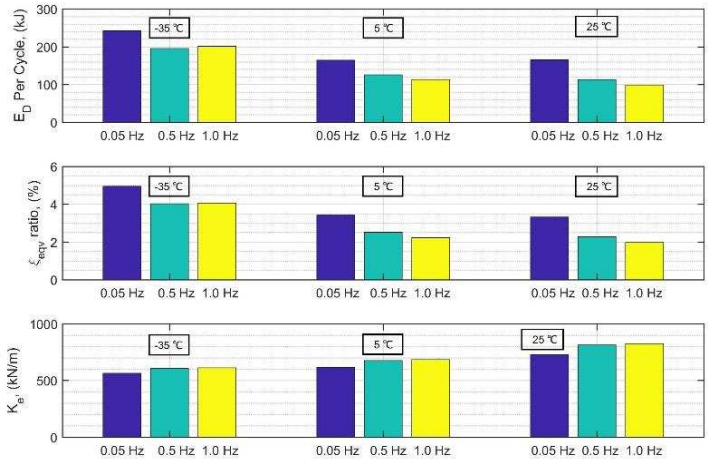


Figure 3. Variation of energy dissipation per cycle, equivalent viscous damping, and equivalent stiffness with loading frequency

Numerical Analyses

In order to explore potential use of high damping SMAs in mitigating response of steel frame buildings subjected to earthquake loads, numerical analyses on a four-story steel building are conducted.

Modeling of NiTiHfPd SMAs

To model hysteretic response of NiTiHfPd SMAs at different temperatures, a mechanical model is proposed in Open System for Earthquake Engineering Simulation (OpenSees) [10]. The model consists of two self-centering materials placed in parallel as shown in Fig. 4 is proposed. The use of two self-centering element instead of one provides more accurate modeling of the material response, especially for inner loops. Since the SMAs will be subjected to dynamic loading during an earthquake, the experimental responses of SMAs at 1 Hz are used for the numerical modeling. The selected parameters of the proposed model under the three temperatures of 25°C, 5°C and -35°C are given in Table 1. Fig. 5 shows the hysteretic curves predicted by the proposed model and experimental response at each temperature. It can be seen that the proposed model can predict the response of NiTiHfPd SMA material very well.

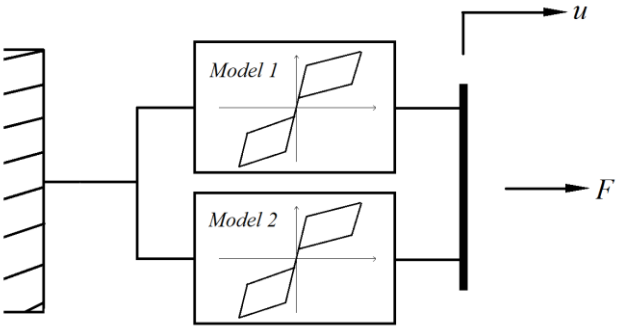
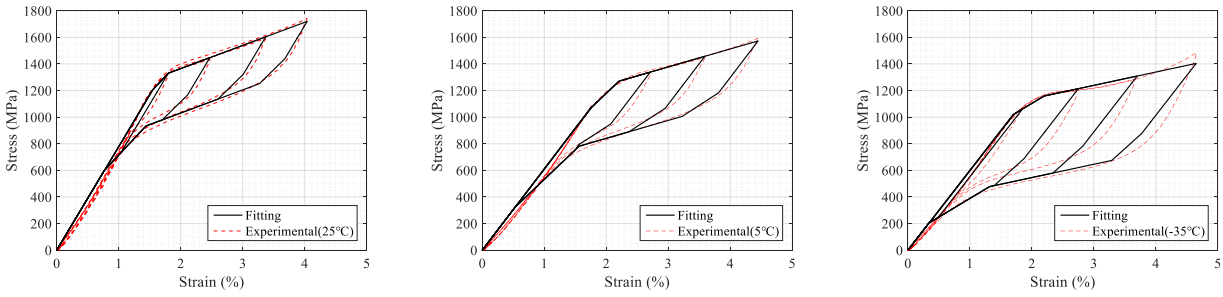


Figure 4. Proposed SMA model



(a) (b) (c)

Figure 5. Experimental stress-strain curves and model predictions at temperature of (a) 25°C, (a) 5°C and (c) -35°C

Table 1. Parameters of proposed SMA model

Temperature	25°C		5°C		-35°C	
Model	1	2	1	2	1	2
Initial stiffness (MPa/%)	370	410	234.4	377	370	230
Post-transformation stiffness (MPa/%)	87	87	67.4	67.4	50	50
Forward transformation stress (MPa)	570	738	410.2	829.4	629	505
Ratio of forward to reverse activation stress (β)	0.50	0.20	0.70	0.29	0.80	0.40

Building Models

Case-Study Building

The prototype steel frame building selected for numerical simulations is designed as an office building located on soil type D in Los Angeles. The structural system consists of steel special moment resisting frame (MRF) designed with fully restrained reduced beam sections and connected with partial restrained gravity frame, which is designed in accordance with LRFD specifications, IBC (2003), SEI/ASCE-02 and ASIC (2002) design provisions. The plan and elevation of the East-West direction of the building are shown in Fig. 6. The structure is classified as Category II and the Maximum Considered Earthquake spectral response acceleration is 1.5g at short periods (S_S) and 0.9g at 1 second period (S_1). The design spectral acceleration parameters S_{MS} and S_{M1} are 1.0g and 0.6g. More details of the prototype frame can be found in Lignos [11]. Two special MRF bays and two additional gravity frame bays on the perimeter as shown in Fig. 6 (b) is modeled using the OpenSees platform.

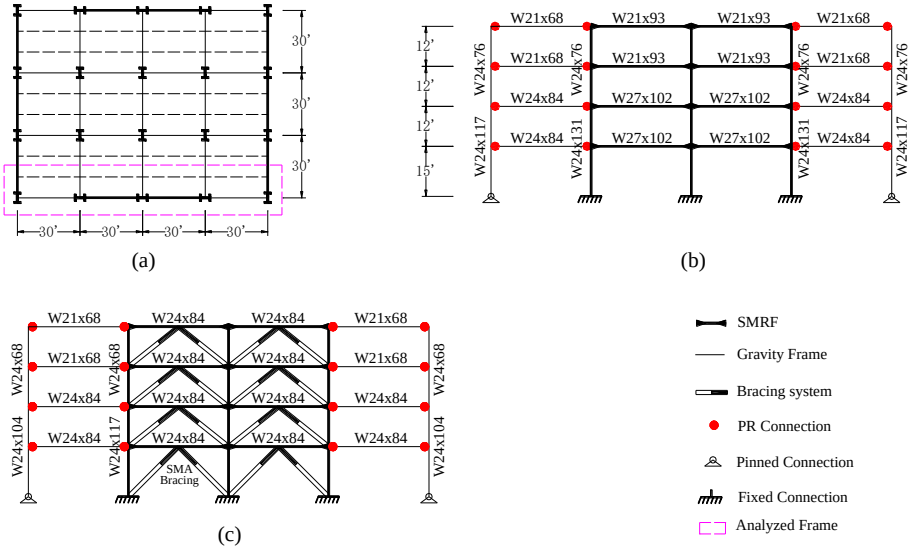


Figure 6. Structural model illustration: (a) Plan view, and elevation views of (b) SMRF and (c) SMA-braced frame.

SMA-braced Frame

In this section, the design of steel frames with SMA bracing systems is discussed. First, an SMA-braced frame is designed assuming the room temperature (25℃) properties of SMAs such that it has comparable strength and stiffness with the original SMRF. To achieve this, the strength of the SMRF is reduced by selecting smaller beam and column section sizes for the frame system such that the reduced strength frame has a base shear capacity equal to about 75% of the base shear capacity of the original SMRF and the selected frame sections satisfy the strength requirements of ASCE 7-10 and ANSI/AISC 360-10. Then, the chevron bracing configuration for SMA braces is adopted and SMA braces are installed at each bay at each story of moment resisting frame as shown in Fig. 6 (c) to satisfy the drift requirements, which is confirmed from through nonlinear response history analyses method.

To investigate the effect of the ambient temperature on seismic performance of SMA braced frames, two additional sets of the brace properties under the temperature of 5℃ and -35℃ have been derived. Note that the geometric dimensions of SMA braces remain the same at each tempereature but the structural properties such as initial stiffness and yield force of the bracing system varies for different temperatures as shown in Table 2 since the mechanical response of the SMAs changes with temperature as discussed earlier. A total of three sets of SMA brace parameters under the temperature of 25°C, 5°C and -35°C are considered. Note that the geometric properties of the SMA braces installed at the 1st and 2nd floors are the same but they are different than those at the 3rd and 4th floors.

Ground Motions

Three sets of SAC ground motions for Los Angeles are used in the numerical simulations. The selected ground motion records are representative of three different hazard levels with a probability of exceedance of 50%, 10% and 2% in 50 years, corresponding to return periods of 72, 475, and 2475 years, respectively. Each set of the ground motions consist of 10 pairs of orthogonal records (i.e. 20 ground motion records). More details concerning individual component information and scaling of the records can be found in FEMA-355C.

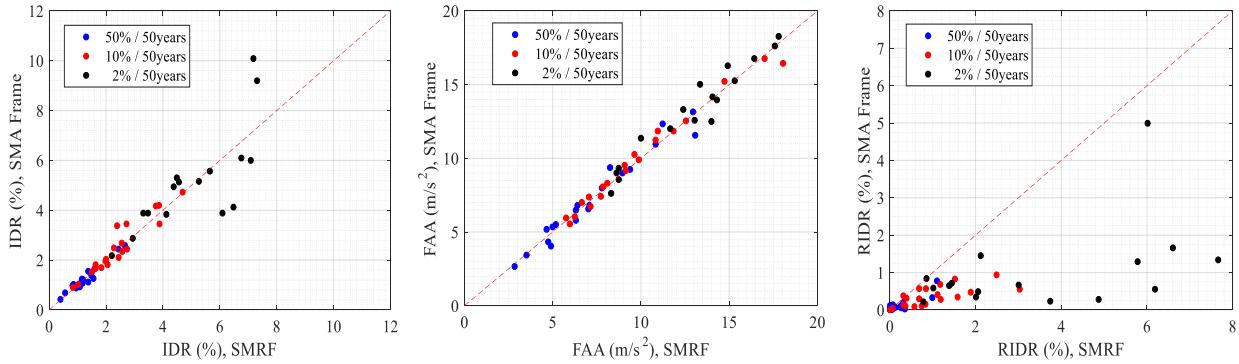
Table 2. SMA brace properties

Temperature	SMA brace	Story	SMA Length (mm)	SMA Area (mm^2)	Initial Stiffness (kN/mm)	Post-yield Stiffness (kN/mm)	Yield Displacement (mm)	Yield Force (kN)	β
25℃	Brace-I	1-2	3300	150	3.55	0.8	50.82	180	0.33
	Brace-II	3-4	2900	150	4.04	0.9	44.66	180	0.33
5℃	Brace-I	1-2	3300	150	2.78	0.61	57.75	160	0.41
	Brace-II	3-4	2900	150	3.16	0.7	50.75	160	0.41
-35℃	Brace-I	1-2	3300	150	2.73	0.45	56.10	153	0.64
	Brace-II	3-4	2900	150	3.10	0.52	49.30	153	0.64

Comparative Seismic Performance Assessment for SMA-braced Frame

Nonlinear response history analyses are carried out for SMRF and SMA-braced Frame (assuming design temperature of 25°C) under a total of 20 ground motions scaled to three

different seismic intensity levels. Fig. 7 compares the maximum inter-story drift ratio (IDR), maximum floor absolute acceleration (FAA) and maximum residual inter-story drift ratio (RIDR) for SMRF and SMA-braced Frame at different seismic intensity levels. In addition, Table 3 shows the median values of IDR, FAA and RIDR under 20 ground motions at each intensity level. The results reveal that the SMA-braced frame shows similar seismic performance in terms of IDR and FAA under three different levels intensities. However, the SMA-braced Frame effectively reduces the residual drifts at the seismic intensity levels of 10/50 and 2/50. In particular, the SMRF exhibit a median RIDR above 4% under ground motion records with a probability of exceedance of 2% in 50 years, while the median RIDR is only 0.69% for the SMA-braced frame.



(a) (b) (c)

Figure 7. Comparison of maximum (a) IDR, (b) FAA and (c) RIDR obtained for SMRF and SMA-braced Frame

Table 3. Median value of structural demand parameters

GM Intensity	Median IDR (%)		Median FAA (m/s^2)		Median RIDR (%)	
	SMRF	SMA-braced Frame	SMRF	SMA-braced Frame	SMRF	SMA-braced Frame
50% /50	1.13	1.07	6.72	6.68	0.09	0.06
10% /50	2.34	2.23	9.12	9.35	0.79	0.33
2% /50	5.88	5.23	14.03	13.14	4.31	0.69

Effect of Temperature on Seismic Performance of SMA-braced Frame

Static pushover analysis

To investigate the effect of temperature on the response of SMA-braced frame buildings, static pushover analyses at three different temperatures are conducted first. The pushover load pattern forces are distributed in proportion to the lateral force prescribed in ASCE 7-10. Table 4 presents the related dynamic and mechanical properties of the SMA-braced frame buildings at different ambient temperature. In table, T_1 is the fundamental period of vibration, θ_y is the roof drift at frame yielding, C_{max} is maximum frame strength coefficient (peak base shear force normalized by weight), α is post-yield stiffness ratio and μ_T is period-based ductility [12]. The pushover curves of the frame at different temperatures are shown in Fig. 8. It can be seen that the strength

and initial stiffness of SMA-braced frames decrease with a decrease in ambient temperature. However, the variation in these properties is more prominent when the temperature reduces from 25°C to 5°C compared to those observed for a temperature change from 5°C to -35°C.

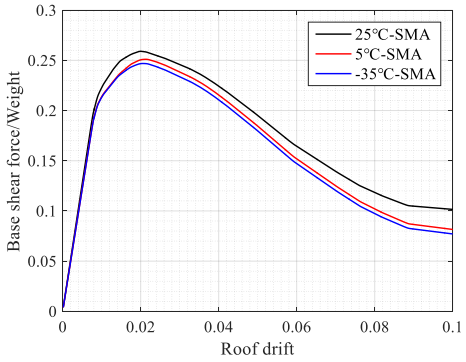


Figure 8. Pushover curves of the building models

Table 4. Dynamic and mechanical properties of the building models

Frame	T_1	θ_y	C_{max}	α	μ_T
SMA_25℃	1.265	0.078	0.259	0.237	4.51
SMA_5℃	1.289	0.083	0.251	0.198	4.11
SMA_-35℃	1.290	0.083	0.247	0.198	4.07

Nonlinear dynamic analysis

Additional nonlinear dynamic analysis are carried out on the SMA-braced frame assuming an outdoor (and bracing) temperature of 5°C and -35°C under each of 20 ground motions scaled to three different intensity levels. The median values of IDR, FAA and RIDR at different temperatures under seismic intensity levels of 50/50, 10/50 and 2/50 are summarized in Table 5. The results illustrate that the temperature have a very small influence on the median structural demand parameters. The largest variation in the response with temperature is observed for the RIDR at intensity level of 2/50, resulting in an increase from 0.69% at 25°C to 0.95% at -35°C.

Table. 5 Median values of structural demand parameters

GMs Intensity	Median IDR (%)			Median FAA (m/s^2)			Median RIDR (%)		
	25℃	5℃	-35℃	25℃	5℃	-35℃	25℃	5℃	-35℃
50% /50	1.07	1.07	1.23	6.68	6.57	6.57	0.064	0.065	0.061
10% /50	2.23	2.31	2.33	9.35	9.15	9.14	0.328	0.369	0.391
2% /50	5.23	5.25	5.12	13.14	13.33	13.15	0.689	0.829	0.950

Conclusions

In this paper, NiTiHfPd alloy is employed as a bracing system in a steel frame building to provide re-centering and energy-dissipating capabilities. First, experimental tests on NiTiHfPd

alloys that have ultra-high strength, large damping capacity, and wide operating temperature range are discussed. Then, a case-study steel building is selected and modeled for numerical investigations. The selected steel moment resisting frame building is also designed and modeled with SMA bracing system such that the SMA-braced frame has comparable strength and stiffness with the original SMRF. Nonlinear response history analyses on conventional SMRF and SMA-braced frame are conducted at different seismic intensity levels using a set of 20 ground motion records. The results indicate that the residual story drifts can significantly be reduced when the steel building are designed with SMA-bracing systems. It is also found that changing temperature between -35°C and 25°C does not affect the performance of NiTiHfPd SMA bracing systems.

Acknowledgments

This material is based upon the work supported by the National Science Foundation under Grant Number CMMI-1538770.

References

1. Alam, M.S., Youssef, M.A. and Nehdi, M. Utilizing shape memory alloys to enhance the performance and safety of civil infrastructure: a review. *Canadian Journal of Civil Engineering* 2007; **34** (9): 1075-1086.
2. Cortés-Puentes WL, Palermo D. SMA tension brace for retrofitting concrete shear walls. *Engineering Structures* 2017; **140**:177-88.
3. Ozbulut OE, Silwal B. Performance assessment of buildings isolated with S-FBI system under near-fault earthquakes. *Smart Structures and Systems* 2016;**17**(5):709-24.
4. Speicher MS, DesRoches R, Leon RT. Investigation of an articulated quadrilateral bracing system utilizing shape memory alloys. *Journal of Constructional Steel Research* 2017;**130**:65-78.
5. Silwal, B., Michael, R. J., and Ozbulut, O. E. A superelastic viscous damper for enhanced seismic performance of steel frame structures. *Engineering Structures* 2015; **105**, 152-164.
6. Ozbulut, O. E., Hurlebaus, S., and DesRoches, R. Seismic response control using shape memory alloys: A Review. *Journal of Intelligent Material Systems and Structures* 2011; **22**, 1531-1549.
7. Ozbulut, O. E., and Hurlebaus, S. Neuro-fuzzy modeling of temperature- and strain-rate-dependent behavior of NiTi shape memory alloys for seismic applications. *Journal of Intelligent Material Systems and Structures* 2010; **21**, 837-849.
8. Acar, E., Ozbulut, O. E., and Karaca, H. E. Experimental investigation and modeling of the strain rate and temperature dependent superelastic response of a high performance SMA. *Smart Materials and Structures* 2015; **24** (7), 075020, 1-12.
9. Saedi, S., Dizaji, F. S., Ozbulut, O. E., and Karaca, H. E. Structural vibration control using high strength and damping capacity shape memory alloys. *Dynamics of Civil Structures, Volume 2: Proceedings of the International Modal Analysis Conference*, Garden Grove: CA, 2017.
10. OpenSees. *Open System for Earthquake Engineering Simulation - Home Page*. April 1, 2014, http://opensees.berkeley.edu/.
11. Lignos, D.G. and Krawinkler, H. Sidesway collapse of deteriorating structural systems under seismic excitations, Rep.No.TB 177. *The John A. Blume Earthquake Engineering Research Center*. Stanford University: CA, 2012.
12. FEMA P695. *Quantification of Building Seismic Performance Factors*. Washington, D.C: Federal Emergency Management Agency, 2009.